



HAL
open science

Dynamic optimisation of the aroma production in brewing fermentation

Ioan-Cristian Trelea, Mariana Titica, Georges Corrieu

► **To cite this version:**

Ioan-Cristian Trelea, Mariana Titica, Georges Corrieu. Dynamic optimisation of the aroma production in brewing fermentation. *Journal of Process Control*, 2004, 14 (1), pp.1-16. 10.1016/S0959-1524(03)00007-6 . hal-01537106

HAL Id: hal-01537106

<https://agroparistech.hal.science/hal-01537106>

Submitted on 16 Jun 2017

HAL is a multi-disciplinary open access archive for the deposit and dissemination of scientific research documents, whether they are published or not. The documents may come from teaching and research institutions in France or abroad, or from public or private research centers.

L'archive ouverte pluridisciplinaire **HAL**, est destinée au dépôt et à la diffusion de documents scientifiques de niveau recherche, publiés ou non, émanant des établissements d'enseignement et de recherche français ou étrangers, des laboratoires publics ou privés.

1 **Dynamic optimisation of the aroma production in brewing**

2 **fermentation**

3 Ioan Cristian TRELEA¹✉, Mariana TITICA², Georges CORRIEU¹

4 ¹UMR Génie et Microbiologie des Procédés Alimentaires, 78850 Thiverval-Grignon, France

5 E-mail: trelea@grignon.inra.fr

6 ²CESAME, UCL Bâtiment Euler, Avenue Georges Lemaître 4-6, B-1348, Louvain la Neuve, Belgium

7 **Abstract**

8
9 Several key compounds for the final beer flavour (higher alcohols, esters, vicinal diketones) are produced during
10 the alcoholic fermentation phase. The paper demonstrates the possibility of obtaining various desired final aroma
11 profiles and reducing the total process time using dynamic optimisation of three control variables: temperature,
12 top pressure and initial yeast concentration in the fermentation tank. The optimisation is based on a sequential
13 quadratic programming algorithm, on a dynamic model of the alcoholic fermentation and on an aroma
14 production model. The robustness of the optimal control profile with respect to model uncertainty is discussed.

15 **Keywords**

16 Beer, aroma compounds, constrained non-linear optimal control, model uncertainty

17 **Introduction**

18
19 The alcoholic fermentation is an important stage in the beer production process. During this phase, fermentable
20 sugars present in the brewing wort are transformed to ethanol and several aroma compounds important for the
21 final beer flavour are produced. The contribution of the alcoholic fermentation phase to the final beer flavour
22 depends on the wort composition, on the yeast strain and on the operating conditions. Industrial operating
23 conditions for most existing beer brands were determined empirically and are confidential. The aim of this work
24 is to demonstrate the possibility of optimising the fermentation temperature profile, the top pressure profile and
25 the initial yeast concentration based on organoleptic and economic criteria. The organoleptic criterion takes into
26 account target concentrations of the following compounds believed to be important for the final beer flavour [1]:
27 two higher alcohols (isoamyl alcohol and phenyl ethanol), three esters (ethyl acetate, ethyl hexanoate and
28 isoamyl acetate) and one vicinal diketone (diacetyl). The economic criterion is based on process time
29 minimisation.

30 Previous work on the optimisation of the brewing process was concerned with the computation of the
31 temperature profile alone. Gee and Ramirez [2] used Pontryagin's minimum principle for the temperature
32 profile optimisation which insured a minimum fermentation time and a maximum ethanol production. Not
33 surprisingly, they found that the fermentation temperature take its maximum possible value at any time. This
34 purely economic optimum could be anticipated from the existing knowledge of the alcoholic fermentation
35 process but is not used in practice because of its undesired effect on the aroma composition. Andres-Toro
36 *et al.* [3] used an optimisation technique based on genetic algorithms and introduced the idea of aroma targets
37 (for ethyl acetate and diacetyl) in addition to fermentation time minimisation. They obtained a non-trivial
38 temperature profile where high temperatures were still favoured, however.

39 The present contribution is an extension and a generalisation of the results of Titica *et al.* [4]. Dynamic
40 optimisation is used to compute flexible control profiles instead of two-stage controls considered previously.
41 Limitations of the process model that made it unsuitable for simulation in time-varying operating conditions
42 were removed. The possibility of reducing the fermentation time substantially without altering the final aroma
43 profile was demonstrated for a beer previously obtained in constant operating conditions. The feasibility (using a
44 single yeast strain and wort composition) of four commercial beer aroma profiles is discussed and the limitations
45 of the aroma control using the three considered operating conditions alone are pointed out. Finally, the
46 robustness of the final aroma concentrations and of the optimal operating conditions with respect to unavoidable
47 modelling errors is analysed.

48 **Materials and methods**

49 ***Experimental***

50 The alcoholic fermentation and the aroma production models were built and validated on data coming from nine
51 laboratory scale experiments. Experiments were carried out in a 15 L, 0.5 m high, stainless steel bioreactor (LSL
52 Biolafitte, France) filled with 12 L of wort, under gentle agitation (100 rpm). Preliminary experiments showed
53 that mechanical agitation was needed to compensate the absence of the natural agitation that occurs in large scale
54 brewing (10 m high tanks or higher) due to CO₂ release. The lager wort and the industrial yeast strain,
55 *Saccharomyces cerevisiae* var. *uvarum*, were provided by the Institut Français de Brasserie et Malterie (IFBM,
56 France). The conditions of the experimental runs R1 to R4 and R6 to R9 were selected according to a 2³
57 experimental design. The three factors were the fermentation temperature (10 and 16°C), the top pressure (50
58 and 800 mbar) and the initial yeast concentration (5 and 20 million cells/mL). The run R5 was performed in
59 intermediate operating conditions (13°C, 450 mbar and 10 million cells/mL).

60 The concentrations of ethanol, isoamyl alcohol, phenyl ethanol, ethyl acetate, ethyl hexanoate and isoamyl
61 acetate were determined by gas chromatography [5] coupled with mass spectrometry in the case of diacetyl [6].
62 The evolved carbon dioxide was recorded with a gas meter (Schlumberger, France), with a resolution better than
63 0.5% of the total amount of gas produced in each experiment. The measurements describing the alcoholic
64 fermentation (ethanol, wort density, CO₂ production, refractive index and fermentable sugar concentration) were
65 reconciled using well-established stoichiometric relationships [7]. The yeast cell concentration was determined
66 with a particle counter (Coulter Z1, Coultronics, France). Three counts were performed at 3 and 3.5 µm and the
67 logarithmic average of the six counts was taken.

68 ***Alcoholic fermentation model***

69 The optimisation of the operating conditions with respect to the specified criterion is an iterative process. In each
70 iteration candidate solutions are tested using a process model. The process model used in this work consisted in
71 an alcoholic fermentation model coupled with an aroma production model.

72 The alcoholic fermentation model is a modified version of a previously reported one [8]. The main modification
73 concerns the description of the CO₂ transfer between the wort and the headspace. In [8] it was assumed that CO₂
74 was dissolved in the wort until saturation and released afterwards. This assumption was reasonable for constant
75 operating conditions, but seems questionable in the dynamic optimisation context when variable temperature and

76 top pressure profiles are usually obtained. The stated assumption was replaced by a rigorous mass balance of the
 77 CO₂ in the wort and in the headspace and a mass balance of the air in the headspace. Solubility of the air (N₂ and
 78 O₂) in the wort was found negligible as far as the mass balance was concerned.

79 The alcoholic fermentation can be described equivalently by the fermentable sugar consumption, ethanol
 80 production, wort density decrease or CO₂ production [7]. The CO₂ was selected because it is the most convenient
 81 variable to be measured on-line [9][10]. The model was constructed by analogy with classical microbial growth
 82 kinetics with substrate limitation and product inhibition:

$$83 \quad \frac{dC_p(t)}{dt} = v(\theta(t), C_d(t)) \cdot \frac{S(t)}{K_S + S(t)} \cdot \frac{1}{1 + (E(t)/K_E)^2} \cdot (C_p(t) + K_X X_0) \quad (1)$$

$$84 \quad C_p(0) = 0 \quad (2)$$

$$85 \quad E(t) = Y_{E/C} C_p(t) \quad (3)$$

$$86 \quad S(t) = S(0) - Y_{S/C} C_p(t) \quad (4)$$

87 The rate of the alcoholic fermentation was described by the rate of CO₂ production dC_p/dt . Simultaneously,
 88 ethanol (E) is produced and fermentable sugars (S) are consumed, with constant yields ($Y_{E/C}$ and $Y_{S/C}$
 89 respectively). The initial fermentation rate, when $C_p = 0$, is proportional to the initial yeast concentration X_0 .

90 The “specific” fermentation rate v was expressed as [11]:

$$91 \quad v(\theta, C_d) = K_v \exp(K_{v\theta}(\theta - \theta_{typ}) - K_{vC}(C_d - C_{d,typ})) \quad (5)$$

92 For small temperature variations ($\pm 3K$) compared to the typical absolute fermentation temperature (286K), the
 93 given relationship is a close approximation of the Arrhenius law. A similar dependence was assumed for the
 94 dissolved CO₂ (C_d). The “typical” temperature and dissolved CO₂ values are those of the central point of the
 95 experimental design (run R5) and correspond to usual values for lager beer making. For modelling purposes, it
 96 was assumed that the produced CO₂ (C_p) is transferred into the solution, because of the large contact area
 97 between the yeast cells and the wort. The mass transfer between the solution (C_d) and the headspace (C_h),
 98 depends on the partial CO₂ pressure in the headspace (p_c) and on the tank geometry and agitation through a
 99 kinetic constant (τ):

$$100 \quad \frac{dC_d(t)}{dt} = \frac{dC_p(t)}{dt} - \frac{1}{\tau} [C_d(t) - C_{sat}(\theta(t), p_c(t))] \quad (6)$$

$$101 \quad C_d(0) = 0 \quad (7)$$

102 C_{sat} is the equilibrium CO₂ concentration in the wort at a given temperature (θ) and at a given partial headspace
 103 pressure (p_c). It was determined from tables provided by Institut Français de Brasserie et Malterie and
 104 approximated by the following empirical formula:

$$105 \quad C_{sat}(\theta, p_c) = K_C p_c \frac{\theta + \theta_{abs}}{\theta_{abs}} e^{-K_{C\theta}\theta} \quad (8)$$

106 The evolution of the CO₂ concentration in the headspace (C_h) is given by :

$$107 \quad \frac{dC_h(t)}{dt} = \frac{\gamma}{\tau} [C_d(t) - C_{sat}(\theta(t), p_c(t))] - \frac{\gamma C_h(t)}{C_h(t) + C_a(t)} \Phi_g(t) \quad (9)$$

$$108 \quad C_h(0) = 0 \quad (10)$$

109 where γ is the ratio of the wort volume to the headspace volume, C_a is the air concentration and Φ_g the total gas
 110 outflow rate (CO₂ + air). The CO₂ outflow rate is proportional to the CO₂ mass fraction in the headspace. The air
 111 concentration in the headspace diminishes with a rate proportional to the air mass fraction:

$$112 \quad \frac{dC_a(t)}{dt} = -\frac{\gamma C_a(t)}{C_h(t) + C_a(t)} \Phi_g(t) \quad (11)$$

$$113 \quad C_a(0) = \frac{p_{atm} M_a}{R(\theta(0) + \theta_{abs})} \quad (12)$$

114 The partial CO₂ (p_c) and air (p_a) pressures were calculated using the perfect gas law. The technologically
 115 important variable is the total pressure (p):

$$116 \quad p_c = \frac{C_h}{M_c} R(\theta + \theta_{abs}) \quad (13)$$

$$117 \quad p_a = \frac{C_a}{M_a} R(\theta + \theta_{abs}) \quad (14)$$

$$118 \quad p = p_c + p_a \quad (15)$$

119 where R is the perfect gas constant, M_c is the CO₂ molar mass and M_a is the equivalent molar mass of the air.

120 The parameter values of the alcoholic fermentation model are reported in Table 1. The differences with
 121 previously reported values [8][12] are due to the way in which the dissolved carbon dioxide was estimated.

122 **Aroma production model**

123 A mathematical model for some aroma compounds produced during the alcoholic fermentation, and considered
 124 important for the final beer flavour, was reported previously [11][12]. The same model was used for optimal
 125 control, with the following modifications: (i) In the new version, the operating conditions affect the yields versus
 126 CO₂ in a multiplicative, rather than additive way. (ii) The two-phase yield for the ester production was replaced
 127 by a single-phase, monotonically increasing yield. (iii) The model parameters were identified based on the whole
 128 pool of experiments, rather than separately for each experiment. This allowed a statistical analysis of the
 129 reliability of the parameter estimates. (iv) Parameters not significantly different from zero were removed from
 130 the model, i.e. set to exactly zero.

131 **Higher alcohols.** Two higher alcohols were considered in this work, based on their organoleptic thresholds in
 132 beer [1]: the isoamyl alcohol (*IAL*) and the phenyl ethanol (*PHL*). Their production rate was related to the
 133 alcoholic fermentation rate, with yields ($Y_{i/C}$) depending on the operating conditions: temperature (θ), dissolved
 134 CO₂ (C_d) and initial yeast concentration in the wort (X_0):

$$135 \quad \frac{dA_i(t)}{dt} = Y_{i/C}(\theta(t), C_d(t), X_0) \frac{dC_p(t)}{dt} \quad i \in \{IAL, PHL\} \quad (16)$$

$$136 \quad A_i(0) = 0 \quad (17)$$

$$137 \quad Y_{i/C}(\theta, C_d, X_0) = W_{i,1} \exp[W_{i,2}(\theta - \theta_{typ}) + W_{i,3}(C_d - C_{d,typ}) + W_{i,4}(X_0 - X_{0,typ}) \\ + W_{i,5}(\theta - \theta_{typ})(C_d - C_{d,typ}) + W_{i,6}(\theta - \theta_{typ})(X_0 - X_{0,typ}) \\ + W_{i,7}(C_d - C_{d,typ})(X_0 - X_{0,typ}) + W_{i,8}(\theta - \theta_{typ})(C_d - C_{d,typ})(X_0 - X_{0,typ})] \quad (18)$$

138 **Esters.** The three selected esters were the ethyl acetate (*ETA*), the ethyl hexanoate (*ETX*) and the isoamyl acetate
 139 (*IAA*). Their production rate was related to the alcoholic fermentation rate, as in the case of higher alcohols, but
 140 the yield increased with fermentation progress:

$$141 \quad \frac{dA_i(t)}{dt} = Y_{i/C}(\theta(t), C_d(t), X_0) C_p(t) \frac{dC_p(t)}{dt} \quad i \in \{ETA, ETX, IAA\} \quad (19)$$

$$142 \quad A_i(0) = 0 \quad (20)$$

143 The effect of the operating conditions on the yields ($Y_{i/C}(\theta, p, X_0)$) had the same mathematical expression as in the
 144 case of the higher alcohols (Equation 18).

145 **Vicinal diketones.** The two important diketones in beer are the diacetyl and the pentanedione. In the considered
 146 experiments, the pentanedione concentration was always lower than the organoleptic threshold [12] and hence
 147 only the diacetyl model was considered for the optimal control. A detailed analysis of this model was given
 148 previously [12]. The diacetyl was simultaneously produced and reduced during the alcoholic fermentation:

$$149 \quad \frac{dA_{DIA}(t)}{dt} = Y_{DIA/C}(t) \frac{dC_p(t)}{dt} - W_{DIA,1} \exp[W_{DIA,2}(\theta - \theta_{typ})] \quad (21)$$

$$150 \quad A_{DIA}(0) = 0 \quad (22)$$

151 The production yield ($Y_{DIA/C}$) asymptotically decreased to zero. An empirical relationship describing this
 152 behaviour was established:

$$153 \quad \frac{dY_{DIA/C}(t)}{dt} = -W_{DIA,3} \frac{dC_p(t)}{dt} Y_{DIA/C}(t) \quad (23)$$

$$154 \quad Y_{DIA/C}(0) = W_{DIA,4} \quad (24)$$

155 **Statistical significance of the model coefficients.** The significance test was based on the so-called Mallows
 156 statistic, which establishes a trade-off between the fit to experimental data and the model complexity, i.e. number
 157 of adjustable parameters [14]. This criterion says that a parameter should be retained in the model only if it
 158 reduces the residual variance sufficiently compared to the estimated measurement variance. For each aroma
 159 compound (i), the Mallows statistic (I_i) was minimised over the various combinations of n_i nonzero parameters:

$$160 \quad I_i = \frac{1}{\sigma_i^2} \sum_k (A_i(t_k) - a_i(t_k))^2 + 2n_i \quad i \in \{ETA, ETX, IAA, IAL, PHL, DIA\} \quad (25)$$

161 Here $a_i(t_k)$ are the measured concentrations and $A_i(t_k)$ are the concentrations predicted by the model with n_i
 162 nonzero parameters. The measurement variance σ_i^2 was estimated as the residual variance of the complete
 163 model, with all nonzero parameters.

164 The numeric values of the coefficients appearing in the aroma production model, together with their confidence
 165 limits, are reported in the Table 2.

166 **Optimal control problem**

167 The optimal control of the fermentation process consisted in the selection of the operating conditions that
 168 minimised an overall criterion Q , which reflected the desired product quality and plant operation mode.
 169 Additional requirements were introduced via a set of constraints that admissible solutions must satisfy. The
 170 operating conditions considered in this work are the wort temperature θ , controlled by the cooling rate Φ_θ , the

171 top pressure p , controlled by the gas outflow rate Φ_g , the initial yeast concentration in the wort X_0 , and the total
 172 fermentation time t_f . The optimal control problem is stated as:

$$173 \quad \{t_f, \Phi_\theta(t)_{t \in [0, t_f]}, \Phi_g(t)_{t \in [0, t_f]}, X_0\} = \arg \min Q \quad (26)$$

174 The “arg min” symbol means the “the values which minimise”. The optimisation criterion and the constraints are
 175 detailed below.

176 **Optimisation criterion**

177 The considered problem is a multiobjective optimisation: approaching the five aroma targets as close as possible,
 178 reducing the final diacetyl concentration and the total processing time, as well as smoothing out the temperature
 179 and the top pressure profiles. The overall optimisation criterion is a weighted sum of the nine partial criteria. The
 180 weights specify the desired trade-offs between possibly conflicting objectives. In order to simplify the selection
 181 of the weights, all partial criteria were scaled by physically meaningful quantities. Thus, the partial criteria and
 182 the associated weights are dimensionless quantities of order of unity.

183 **Approaching the aroma targets.** The final concentrations of the five aroma compounds, believed to be
 184 important for the final beer flavour, have to be as close as possible to their respective targets:

$$185 \quad Q_i = W_i \frac{(A_i(t_f) - A_{i,trg})^2}{A_{i,tol}^2}, \quad i \in \{ETA, ETX, IAA, IAL, PHL\} \quad (27)$$

186 Here Q_i is the partial criterion associated to the aroma compound i , W_i is the associated weight, $A_i(t_f)$ is the aroma
 187 concentration at the end of the fermentation, $A_{i,trg}$ is the target concentration, and $A_{i,tol}$ is the accepted tolerance.
 188 Since there is no point in trying to approach the target closer than either the model accuracy or the perceived
 189 difference, the tolerance was selected as:

$$190 \quad A_{i,tol}^2 = \sigma_i^2 + A_{i,org}^2 \quad (28)$$

191 where σ_i is the model prediction accuracy (Table 2) and $A_{i,org}$ is the organoleptically significant difference in the
 192 concentration of the compound i taken as 10% of the organoleptic threshold of the considered compound in beer
 193 [1]. An alternative way of expressing the tolerance would be using the largest of the two values σ_i and $A_{i,org}$. The
 194 tolerance provides a natural scaling of the associated optimisation criterion.

195 **Minimising the diacetyl concentration.** Diacetyl is an undesired compound in the finished beer. No target was
 196 defined for this compound because the lowest possible value is desired in practice (ideally zero). Minimisation of
 197 the diacetyl concentration at the end of the main fermentation is an economically important goal, since it may
 198 result in the reduction of the cost of the subsequent processing (dedicated “diacetyl rest” and/or lagering phases).
 199 Mathematically, this goal was expressed as:

$$200 \quad Q_{DIA} = W_{DIA} \frac{A_{DIA}(t_f)}{A_{DIA,typ}} \quad (29)$$

201 where $A_{DIA}(t_f)$ is the diacetyl concentration at the end of the alcoholic fermentation and $A_{DIA,typ}$ is a typical value
 202 of the final diacetyl concentration, used as a scaling constant.

203 **Minimising the fermentation time.** The reduction of the processing time is desirable from an economic point of
 204 view. No target value was given for the fermentation time. The optimisation algorithm was free to select the
 205 shortest possible fermentation time compatible with the other requirements:

$$206 \quad Q_t = W_t \frac{t_f}{t_{typ}} \quad (30)$$

207 where t_f is the final fermentation time and t_{typ} is a typical value for the final time, used for scaling.

208 **Smoothing out the temperature and top pressure profiles.** Technologically, a smooth plant operation is
 209 usually desired. Smooth temperature profile requires a smaller peak cooling power. A smooth top pressure
 210 profile avoids discontinuities in the CO₂ outflow, facilitating its recovery. Numerically, penalising zigzagging
 211 profiles favours robust convergence to a global optimum. The smoothing objective was expressed as a penalty of
 212 the curvature (second time derivative) of the temperature and top pressure profiles. For numerical computations,
 213 the profiles were sampled at equally spaced time points. The scaling factors were chosen to make the curvature
 214 criteria invariant with respect to the total fermentation time and to the range of the variables:

$$215 \quad Q_\theta = W_\theta \frac{1}{n_t - 2} \sum_{k=2}^{n_t-1} \left(\frac{\theta_{k+1} - 2\theta_k + \theta_{k-1}}{\theta_{\max} - \theta_{\min}} \right)^2 \quad (31)$$

$$216 \quad Q_p = W_p \frac{1}{n_t - 2} \sum_{k=2}^{n_t-1} \left(\frac{p_{k+1} - 2p_k + p_{k-1}}{p_{\max} - p_{atm}} \right)^2 \quad (32)$$

217 Here n_t is the total number of sampling points, θ_k and p_k are wort temperature and total headspace pressure at the
 218 sampling point number k .

219 **Overall optimisation criterion.** The overall optimisation criterion is the sum of the nine partial criteria. It
 220 reflects the best possible trade-off between generally conflicting optimisation goals:

$$221 \quad Q = \sum_{i \in \{ETA, ETX, IAA, IAL, PHL, DIA, t, \theta, p\}} Q_i \quad (33)$$

222 **Technological constraints**

223 The operating conditions (temperature, top pressure and initial yeast concentration) were limited to the model
 224 validity range, which is the range of the operating conditions of the experimental design that provided data for
 225 model identification and validation. Additionally, the initial top pressure must equal the atmospheric pressure
 226 p_{atm} , since it can be increased only by the CO₂ produced by fermentation:

$$227 \quad \theta(t) \in [\theta_{\min}, \theta_{\max}], \quad t \in [0, t_f] \quad (34)$$

$$228 \quad p(t) \in [p_{atm}, p_{\max}], \quad t \in [0, t_f] \quad (35)$$

$$229 \quad p(0) = p_{atm} \quad (36)$$

$$230 \quad X_0 \in [X_{0\min}, X_{0\max}] \quad (37)$$

231 On most fermentation tanks, the temperature is controlled using a cooling jacket. The associated control variable,
 232 namely the cooling rate Φ_θ , can only be positive since no heating device usually exists. Its amplitude is limited
 233 by the maximum available cooling power or the maximum possible heat transfer rate:

$$234 \quad \Phi_\theta(t) \in [0, \Phi_{\theta\max}], \quad t \in [0, t_f] \quad (38)$$

235 The top pressure is generally controlled by a valve. The corresponding control variable is the outflow gas rate Φ_g ,
 236 which is also positive and limited by the valve diameter:

$$237 \quad \Phi_g(t) \in [0, \Phi_{g\max}], \quad t \in [0, t_f] \quad (39)$$

238 The alcoholic fermentation is considered finished when the residual fermentable sugar concentration reaches a
 239 specified value, corresponding to the so-called wort “attenuation” limit:

$$240 \quad S(t_f) = S_{res} \quad (40)$$

241 This constraint defines the fermentation end time t_f . The residual concentration S_{res} is generally known for a
 242 given wort and yeast strain.

243 Numerical values of the optimal control problem parameters are reported in Table 3. The target aroma
 244 concentrations considered in this work are given in Table 4. The aroma profiles of the five sorts of beer listed in
 245 Table 4 are discussed in the “Results and discussion” section below.

246 **Dynamic optimisation algorithm**

247 The considered optimal control problem is a dynamic one, since the unknown control variables are functions of
 248 time. The optimisation criterion contains linear and quadratic terms in the state variables. The constraints are
 249 linear in the state and control variables, except the top pressure constraint, which involves products of state
 250 variables ($C_d(t)\theta(t)$ and $C_a(t)\theta(t)$). However, the main nonlinearity comes from the dynamic model of the
 251 fermentation process.

252 Taking into account these characteristics of the control problem, a variant of the sequential quadratic
 253 programming (SQP) algorithm was used for solving it [15], coupled with a collocation (time discretisation)
 254 technique [16] and a safeguarded line search based on a “confidence region” method [17]. The main steps of the
 255 algorithm were:

256 **Step 0. Initialisation.** A non-optimal but admissible (with respect to the constraints) solution was determined
 257 before entering the main algorithm. The initial fermentable sugar concentration is determined from the desired
 258 ethanol concentration in the finished beer (E_{trg}):

$$259 \quad S(0) = S_{res} + \frac{Y_{S/C}}{Y_{E/C}} E_{trg} \quad (41)$$

260 Random but admissible set-point profiles were generated for temperature and top pressure. A random admissible
 261 value was generated for the initial yeast concentration. The model equations were solved using simple
 262 proportional controllers to follow the set-points:

$$263 \quad \Phi_\theta(t) = K_{p\theta} (\theta(t) - \theta_{set}(t)) \quad (42)$$

$$264 \quad \Phi_g(t) = K_{pg} (p(t) - p_{set}(t)) \quad (43)$$

265 The fermentation end time (t_f) was determined as the moment when the fermentable sugar concentration fell
 266 below the specified limit (S_{res}). The resulting control variables (cooling rate and gas outflow rate) and the
 267 resulting fermentation end time were used as starting points for the optimisation.

268 **Step 1. Discretisation of the dynamic problem.** Let x be the vector of the $n_x = 12$ state variables and u the
 269 vector of the $n_u = 2$ control variables:

$$270 \quad x = [C_p \quad A_{ETA} \quad A_{ETX} \quad A_{IAA} \quad A_{LAI} \quad A_{PHL} \quad A_{DIA} \quad Y_{DIA/C} \quad \theta \quad C_d \quad C_h \quad C_a]^T \quad (44)$$

$$271 \quad u = [\Phi_\theta \quad \Phi_g]^T \quad (45)$$

272 The state and control variables were sampled at a finite number ($n_t = 49$) of time points [16]. This reduced an
273 infinite-dimensional problem to a finite-dimensional one, which could be handled by a numerical computer. The
274 optimisation criterion, the constraints and the dynamic model equations were discretised on the same time grid.
275 **Step 2. Construction of a local optimisation sub-problem.** The SQP method requires local approximation of
276 the non-linear optimisation problem by a quadratic one with linear constraints, using limited Taylor series
277 expansion. In the standard SQP method the quadratic approximation is made to the Lagrangean function. Its
278 Hessian matrix includes curvature information on both the objective function and the constraints [15]. In this
279 application the Hessian matrix of the objective function alone was used. The objective function being truly
280 quadratic, its second order Taylor series expansion was exact. The discretised dynamic model equations were
281 treated as additional constraints [15]. The limited Taylor series expansion being valid only locally, a limited
282 search region around the current solution was established, using a set of “box” (min-max) constraints [17].
283 **Step 3. Solution of the local optimisation sub-problem.** Commercial software, based on an “active constraint
284 set” method was used to solve the quadratic optimisation problems with linear constraints [18]. This software did
285 not exploit the special structure of the collocation equations and was unable to solve a problem of moderate size
286 ($2 + n_t(n_u + n_x) = 688$). The number of variables was reduced to $2 + n_t n_u + n_x = 112$ by solving the
287 linearized collocation equations explicitly. The reduction step involved a structurally well conditioned and sparse
288 matrix, making the computation both fast and accurate.
289 **Step 4. Convergence test.** The non-linear state equations were solved using the determined control variables.
290 The value of the optimisation criterion was computed and the satisfaction of the constraints was checked. If the
291 control variables, the state variables and the optimisation criterion were modified by less than a pre-specified
292 amount, and if all constraints were satisfied, then calculations were halted. Else a new iteration was made,
293 starting with step 1.
294 The algorithm was always run several (~10) times with various random initialisation in step 0. Robust
295 convergence to the same optimum was observed. Occasionally, local optima in form of zigzagging control
296 profiles were encountered. The control smoothing terms (Equations 31 and 32) were found very useful in
297 avoiding these local optima. A detailed mathematical description of the algorithm is available from the authors
298 on request.

299 **Results and discussion**

300 ***Alcoholic fermentation model validation***

301 The main measured and simulated variables in the alcoholic fermentation model are presented in Figure 1 for the
302 run R5, not used for the identification of the model coefficients. The carbon dioxide evolution rate is predicted
303 reasonably well. The evolution rate is zero for the first 24 hours: during this time period the produced CO₂ is
304 partly dissolved in the wort and partly accumulated in the headspace increasing the top pressure. The top
305 pressure increases until the set-point is reached and then remains constant being controlled by the outflow valve.
306 The partial air pressure remains constant until the outflow valve is opened and then decreases, the air being
307 evacuated from the tank along with the CO₂. The partial CO₂ pressure equals the total one when the air was
308 evacuated completely. The ethanol production, proportional to the cumulated CO₂ production, is predicted
309 almost perfectly in this run. It appears from the model simulation that the dissolved CO₂ exceeds its saturation

310 limit by about 50% during the most active fermentation period (between 50 and 100 hours). Dissolved CO₂
311 could not be measured directly in the considered experiments but this value is consistent with data found in the
312 literature [19] and strongly depends on the tank geometry through the parameter τ in Equations 6 and 9. Taking
313 into account the CO₂ super-saturation is the main evolution of the model considered in this paper compared to
314 previous work [8]. It has a moderate impact on the aroma concentrations predicted by the model, particularly in
315 time-varying operating conditions when the top pressure is decreased quickly.

316 ***Aroma production model validation***

317 Measured and simulated concentrations of the aroma compound considered in this work are reported in Figure 2
318 for the experimental run R5, not used for model derivation. The concentrations of five out of the six compounds
319 are predicted reasonably well taking into account the scatter of the experimental data. The concentration of
320 isoamyl acetate is significantly overestimated, however. This was already the case with previous models [11].
321 The measured final isoamyl acetate concentration in run R5 is one of the lowest among all runs, while the
322 operating conditions have intermediate values. This is probably due to anomalous measurements for this
323 particular experiment: in later runs, carried out in conditions similar to run R5, final isoamyl acetate
324 concentrations close to 1.5 mg/L were obtained. The diacetyl is simultaneously produced and reduced during the
325 fermentation run. The production rate decreases gradually and approaches zero at 50 hours. The diacetyl
326 concentration reaches a maximum when the reduction rate equals the production rate and declines exponentially
327 when the production rate becomes negligible.

328 ***Producing an existing beer at a lower cost***

329 This section illustrates the reduction of the production cost for an existing sort of beer without altering its aroma
330 profile. By “aroma profile” is meant here the set of final concentrations of the two higher alcohols and three
331 esters considered in this work. The target aroma concentrations were those measured at the end of the run R5,
332 that is at the central point of the experimental design. The simulated experiment corresponding to run R5 is
333 shown in Figure 3(A). With constant temperature (13°C), constant top pressure (450 mbar above the atmospheric
334 pressure) and a typical initial yeast concentration (10 million cells/mL) the target aroma profile is reproduced
335 well, illustrating the adequacy of the model. The predicted fermentation time is 121 hours, in agreement with the
336 experimental value (Figures 1 and 2).

337 The result of applying the optimisation algorithm to the same target aroma profile is illustrated in Figure 3(B).
338 The final predicted aroma profile matches the target equally well but the fermentation time is reduced to
339 81 hours, that is by 33%. This is achieved by increasing the average fermentation temperature and the initial
340 yeast concentration. The aromatic equilibrium of the final beer is maintained, however, using variable operating
341 conditions (slightly decreasing temperature and uniformly increasing top pressure) by taking advantage of the
342 time-varying fermentation rate and of the time-varying ester yields. The final diacetyl concentration was the
343 same as in run R5 (0.5 mg/L): the highest diacetyl degradation rate due to higher temperature was compensated
344 by a shorter fermentation time.

345 ***Producing new beer flavours with the same yeast strain and wort***

346 The measured aroma concentrations in four existing beer brands (coded B1 to B4, Table 4) were given as targets
347 to the optimal control algorithm. The results for the beers B2 and B3 are shown in Figure 4. Beer B2 has a
348 relatively high concentration of higher alcohols and a low ester concentration, while the opposite is true for beer
349 B3. Figure 4 shows that both aroma profiles can be achieved using the same wort and yeast strain but different
350 operating conditions: Beer B2 needs a high initial yeast concentration, a high fermentation temperature (except
351 for the final phase) and a bell-shaped top pressure profile, while the aroma profile of beer B3 requires roughly
352 the opposite: low initial yeast concentration, V-shaped temperature profile and a low top pressure for most of the
353 fermentation time. Note that beer B2 is produced much faster than beer B3 (91 hours instead of 152) mainly
354 because of the higher average temperature and of the higher initial yeast concentration. This illustrates the fact
355 that the selected weights in the optimisation criterion (Table 3) favour the reproduction of the desired target
356 aroma profile compared to time minimisation, which is only a secondary objective: for beer B3, the fermentation
357 time was increased as much as needed to obtain the desired final aroma composition.

358 It is expected, however, that not *all* aroma profiles can be reproduced with the given yeast strain and wort, even
359 if the operating conditions are selected optimally in their admissible ranges. Two examples are given in Figure 5
360 for the aroma targets of beers B1 and B4 (Table 4). The difficulty of achieving the aroma profile B1 comes from
361 the fact a low concentration of ethyl hexanoate can not be obtained simultaneously with a high concentration of
362 isoamyl acetate. The sensitivity of these compounds to the operating conditions (coefficients $W_{i,2}$ to $W_{i,8}$,
363 Table 2) are very similar, meaning that their concentrations can not be manipulated independently. The best
364 possible solution found by the optimisation algorithm (Figure 5(A)) is a compromise where the final
365 concentration of isoamyl acetate is lower than required and that of ethyl hexanoate is higher. The concentrations
366 of ethyl acetate and isoamyl alcohol are reproduced correctly, however, and that of phenyl ethanol is in the
367 tolerance domain. The situation is worse for the aroma profile B4 (Figure 5(B)) because the target concentration
368 of ethyl hexanoate is even lower and the concentration of isoamyl acetate even higher. The only compound for
369 which the target is achieved in this case is the isoamyl alcohol.

370 ***Final aroma profile robustness with respect to model uncertainty***

371 Due to the finite amount of experimental data available for model identification and to unavoidable measurement
372 error the beer fermentation model parameters (Tables 2 and 3) can only be determined with limited accuracy.
373 The uncertainty on the model parameters was expressed as a joint probability distribution and determined
374 numerically (based on the so-called local Fisher information matrix) during the model fitting process [20]. The
375 performance robustness was tested for the B2 beer by applying the pre-computed optimal operating conditions
376 (temperature profile, top pressure profile and initial yeast concentration) to 20 models with parameters drawn at
377 random from their respective probability distributions. The 95% confidence domain of the final aroma
378 concentrations is shown in Figure 6(A). The confidence domain was determined as the range between the 2.5
379 and the 97.5 percentile of the calculated values. It appears from Figure 6 that the final aroma concentrations stay
380 within their admissible tolerance limits despite model uncertainty. This is consistent with the selection of the
381 tolerance limits that are always larger than the model accuracy (Equation 28).

382 **Optimal control strategy robustness with respect to model uncertainty**

383 The sensitivity of the optimal control profile to the model uncertainty was investigated for the B3 beer by
384 performing the optimal control calculation for 20 models with parameters drawn at random from their respective
385 probability distributions. The 95% confidence domains of the final aroma concentrations and of the associated
386 operating conditions (temperature, top pressure and initial yeast concentration) are shown in Figure 6(B). The
387 confidence domain was determined as the range between the 2.5 and the 97.5 percentile of the calculated values.
388 It appears that similar optimal control policies are obtained consistently despite model parameter variations. A
389 V-shaped temperature profile, a bell-shaped top pressure profile and a low initial yeast concentration seem to be
390 truly characteristic to the considered combination of yeast strain, wort composition and target aroma profile. The
391 exact values of the operating conditions are not critical, however. For example, in a practical implementation,
392 $\pm 0.5^\circ\text{C}$ variations in the wort temperature, ± 200 mbar variations in the top pressure or ± 0.5 million cells/mL
393 variations in the initial yeast concentration would not affect the final beer flavour significantly.

394 **Conclusion**

395 A dynamic model of the beer fermentation process, including an alcoholic fermentation model and an aroma
396 production model, was designed and validated. It is based on nine fermentation runs with operating conditions
397 (temperature, top pressure and initial yeast concentration) selected according to a 2^3 experimental design. The
398 model was used for the dynamic optimal control of the beer fermentation process. A primary goal was to
399 approach pre-specified final aroma targets (two higher alcohols and three esters simultaneously) as close as
400 possible and a secondary objective was to reduce the fermentation time and the final concentration of an
401 undesired aroma compound (diacetyl).

402 An optimal time-varying control policy allowed the reduction of the fermentation time of an existing sort of
403 beer, previously produced in constant operating conditions, by 33% while preserving the final aroma
404 concentrations of the considered compounds. The optimal control strategy also allowed the reproduction of
405 aroma profiles of two existing commercial beers (with different higher alcohols / esters ratios) by means of the
406 operating conditions alone, i.e. using the same yeast strain and wort. Two other existing aroma profiles could not
407 be reproduced satisfactorily (with the same yeast strain and wort) because some aroma compounds had similar
408 sensitivities to the considered operating conditions and could not be manipulated independently.

409 The sensitivity of the final aroma concentrations and of the optimal control policies with respect to modelling
410 errors was explored numerically by generating random sets of model coefficients from their joint probability
411 distributions estimated during the model identification phase. Achievable aroma profiles stayed within the
412 tolerance limits and consistent optimal control profiles were obtained despite model uncertainty.

413 **References**

- 414 [1] S. Engan, Organoleptic threshold values of some alcohols and esters in beer, *Journal of the Institute of*
415 *Brewing* 78 (1972) 33-36.
- 416 [2] A. Gee, W.F. Ramirez, Optimal temperature control for batch beer fermentation, *Biotechnology and*
417 *Bioengineering* 31 (1988) 224-234.

- 418 [3] B. Andres-Toro, J.M. Giron-Sierra, J.A. Lopez-Orozco, C. Fernandez-Conde, Evolutionary optimisation
419 of an industrial batch fermentation process, ECC'97 European Control Conference, Brussels, Belgium 3
420 (1997) WE-EG5 615.
- 421 [4] M. Titica, I.C. Trelea, A. Cheruy, optimisation of fermentation operating conditions with a view to
422 control beer aroma profile, CAB-8: 8th International Conference on Computer Applications in
423 Biotechnology, June 24-27 (2001) Quebec, Canada
- 424 [5] L.E. Stenroos, K.J. Siebert, M.C. Meilgaard, Gas chromatography determination of beer volatiles by
425 carbon disulphide extraction: improved technology, data handling and interpretation, Journal of the
426 American Society of Brewing Chemists 32 (1976) 4-13.
- 427 [6] S. Landaud, P. Lieben, D. Picque, Quantitative analysis of diacetyl, pentanedione and their precursors
428 during beer fermentation by an accurate GC/MS method. Journal of the Institute of Brewing 104 (1998)
429 93-99.
- 430 [7] I.C. Trelea, L. Latrille, S. Landaud, G. Corrieu, Reliable estimation of the key variables and of their rates
431 of change in alcoholic fermentation, Bioprocess and biosystems engineering 24 (2001) 227-237.
- 432 [8] I.C. Trelea, M. Titica, S. Landaud, E. Latrille, G. Corrieu, A. Cheruy, Predictive modelling of brewing
433 fermentation: from knowledge-based to black-box models. Mathematics and Computers in Simulation 56
434 (2001) 405-424.
- 435 [9] S.I. Daoud, B.A. Searle, On-line monitoring of brewing fermentation by measurement of CO₂ evolution
436 rate, Journal of the Institute of Brewing 96 (1990) 297-302.
- 437 [10] G. Corrieu, I.C. Trelea, B. Perret, On-line estimation and prediction of density and ethanol evolution in
438 the brewery, MBAA Technical Quarterly 37(2) (2000) 173-181.
- 439 [11] M. Titica, S. Landaud, I.C. Trelea, E. Latrille, G. Corrieu, A. Cheruy, Modelling of higher alcohol and
440 ester production kinetics based on CO₂ emission, with a view to beer flavour control by temperature and
441 top pressure. Journal of the American Society of Brewing Chemists, 54(4) (2000) 167-174.
- 442 [12] I.C. Trelea, S. Landaud, L. Latrille, G. Corrieu, Prediction of confidence limits for the diacetyl
443 concentration during beer fermentation, Journal of the American Society of Brewing Chemists 60 (2002)
444 in press.
- 445 [13] M.C. Meilgaard, D.S. Reid, K.A. Wyborski, Reference standards for the beer flavour terminology system.
446 Journal of the American Society of Brewing Chemists, 36 (1982) 119-128.
- 447 [14] C. L. Mallows, Some comments on C_p , Technometrics, 15 (1973) 661-675.
- 448 [15] J.T. Betts, Practical methods for optimal control using nonlinear programming, Society for Industrial and
449 Applied Mathematics, Philadelphia (2001) 190 p.
- 450 [16] W.H. Press, S.A. Teukolsky, W.T. Vetterling, B.P. Flannery, Numerical recipes in C, Chapter 17: Two
451 point boundary value problems, Cambridge University Press, 1997, pp. 762-772.
- 452 [17] P.E. Gill, W. Murray, M.H. Wright, Practical optimisation, Academic Press, London 1981.
- 453 [18] T. Coleman, M.A. Branch, A. Grace, Optimisation toolbox for Matlab: User's guide, The
454 MathWorks Inc., 1999, pp. 2.23-2.32.
- 455 [19] I. Daoud, R. Dyson, J. Irvine, R.C. Cuthbertson, Practical experience of on-line monitoring of evolved
456 CO₂ from production fermenters, Proceedings of the 22nd European Brewing Convention, Zurich, Germany
457 (1989) 323-330.

458 [20] K. Bury, *Statistical distributions in engineering*, Cambridge University Press (1999) pp. 27-48.

Nomenclature

Symbol	Units	Significance
θ	°C	Wort temperature
θ_{abs}	K	Absolute temperature conversion constant
θ_{max}	°C	Maximum allowed fermentation temperature
θ_{min}	°C	Minimum allowed fermentation temperature
θ_{set}	°C	Set-point value for the fermentation temperature
θ_{typ}	°C	Typical fermentation temperature
ν	h ⁻¹	“Specific” CO ₂ production rate
σ_i	mg L ⁻¹	Residual standard deviation of the model for the aroma compound i
τ	h	Rate constant for CO ₂ transfer between wort and headspace
γ	L L ⁻¹	Wort volume to headspace volume ratio
Φ_θ	°C h ⁻¹	Wort cooling rate. For a specified amount of wort, it corresponds to a cooling power
$\Phi_{\theta max}$	°C h ⁻¹	Maximum achievable wort cooling rate.
Φ_g	g L ⁻¹ h ⁻¹	Gas outflow rate from the tank (CO ₂ + air), per litre of wort
$\Phi_{g max}$	g L ⁻¹ h ⁻¹	Maximum achievable gas outflow rate from the tank, per litre of wort
A_{DIA}	mg L ⁻¹	Diacetyl concentration
$A_{DIA,typ}$	mg L ⁻¹	Typical diacetyl concentration at the end of the alcoholic fermentation
A_i	mg L ⁻¹	Concentration of the aroma compound i
$A_{i,org}$	mg L ⁻¹	Organoleptically significant difference in the concentration of the aroma compound i
$A_{i,tol}$	mg L ⁻¹	Tolerance in achieving the concentration of the aroma compound i
$A_{i,trg}$	mg L ⁻¹	Target concentration for the aroma compound i
C_a	g L ⁻¹	Amount of air per litre of headspace
C_d	g L ⁻¹	Dissolved CO ₂ concentration
$C_{d,typ}$	g L ⁻¹	Typical dissolved CO ₂ concentration
C_h	g L ⁻¹	Amount of gaseous CO ₂ per litre of headspace
C_p	g L ⁻¹	Produced CO ₂ per litre of wort
C_{sat}	g L ⁻¹	Dissolved CO ₂ concentration at equilibrium
DIA		Diacetyl
E	g L ⁻¹	Ethanol concentration in the wort
E_{trg}	g L ⁻¹	Target ethanol concentration at the end of the alcoholic fermentation
ETA		Ethyl acetate
ETX		Ethyl hexanoate
I_i	none	Akaike’s information criterion for the aroma compound i
i	none	Index of an aroma compound. One of { ETA , ETX , IAA , IAL , PHL }
IAA		Isoamyl acetate
IAL		Isoamyl alcohol
k	none	Sampling time index

K_v	h^{-1}	“Specific” CO_2 production rate constant
$K_{v\theta}$	$^{\circ}\text{C}^{-1}$	Sensitivity of the CO_2 production rate with respect to temperature
K_{vC}	$\text{g}^{-1} \text{L}$	Sensitivity of the CO_2 production rate with respect to dissolved CO_2 concentration
K_C	g L^{-1}	Dissolved CO_2 constant
$K_{C\theta}$	$^{\circ}\text{C}^{-1}$	Sensitivity of the dissolved CO_2 with respect to temperature
K_E	g L^{-1}	Ethanol inhibition constant
$K_{p\theta}$	h^{-1}	Wort temperature controller parameter
K_{pp}	$\text{g L}^{-1} \text{h}^{-1}$ mbar^{-1}	Top pressure controller parameter
K_S	g L^{-1}	Substrate limitation constant
K_X	$\text{g L}^{-1} (10^6 \text{ cells mL}^{-1})^{-1}$	Initial CO_2 production rate constant
M_a	g mol^{-1}	Equivalent air molar mass
M_c	g mol^{-1}	CO_2 molar mass
n_i	none	Number of nonzero model parameters
n_t	none	Number of time sampling points
n_u	none	Number of control variables
n_x	none	Number of state variables
p	mbar	Total (air + CO_2) top pressure in the fermentation tank
p_a	mbar	Partial air pressure in the headspace
p_{atm}	mbar	Atmospheric pressure
p_c	mbar	Partial CO_2 pressure in the headspace
p_{max}	mbar	Maximum allowed top pressure in the fermentation tank
p_{set}	mbar	Set-point value for the top pressure in the fermentation tank
PHL		Phenyl ethanol
Q	none	Global optimisation criterion
Q_{θ}	none	Partial optimisation criterion for the smoothing of the wort temperature profile
Q_{DIA}	none	Partial optimisation criterion for final diacetyl concentration minimisation
Q_i	none	Partial optimisation criterion associated to aroma compound i
Q_p	none	Partial optimisation criterion for the smoothing of the top pressure profile
Q_t	none	Partial optimisation criterion for the total fermentation time minimisation
R	mbar L mol^{-1} K^{-1}	Perfect gas constant
S	g L^{-1}	Fermentable sugar concentration in the wort
S_{res}	g L^{-1}	Desired residual (final) fermentable sugar concentration in the wort
t	h	Fermentation time since yeast inoculation
t_f	h	Total alcoholic fermentation time
t_{fmax}	h	Maximum allowed total alcoholic fermentation time
t_{typ}	h	Typical duration of the alcoholic fermentation
u		Vector of the control variables

W_θ	none	Weight associated to the smoothing of the wort temperature profile
W_{DLA}	none	Weight associated to the minimisation of the final diacetyl concentration
$W_{DLA,j}$	none	Diacetyl production and reduction model coefficients
W_i	none	Weight associated to the partial optimisation criterion Q_i
$W_{i,j}$	none	Aroma production model coefficient j for compound i
W_p	none	Weight associated to the smoothing of the top pressure profile
W_t	none	Weight associated to the minimisation of the total fermentation time
x		Vector of the state variables
X_0	10^6 cells mL ⁻¹	Initial yeast concentration in the wort
$X_{0\ min}$	10^6 cells mL ⁻¹	Minimum allowed initial yeast concentration in the wort
$X_{0\ max}$	10^6 cells mL ⁻¹	Maximum allowed initial yeast concentration in the wort
$Y_{DLA/C}$	mg g ⁻¹	Diacetyl versus CO ₂ production yield
$Y_{E/C}$	g g ⁻¹	Ethanol versus CO ₂ production yield
$Y_{i/C}$	mg g ⁻¹	Yield of aroma compound i versus CO ₂
$Y_{S/C}$	g g ⁻¹	Fermentable sugar versus CO ₂ yield

Table 1. Numerical values of the parameters in the alcoholic fermentation model

Para	Units	Value (95% confidence limits)	Source
meter			
θ_{abs}	K	273.16	Unit conversion: degrees Celsius to Kelvin
θ_{typ}	°C	13	Central point of the experimental design
τ	h	3	Separate experiment
γ	L L ⁻¹	4	Experimental protocol
$C_{d,typ}$	g L ⁻¹	2.76	Central point of the experimental design, Equation (8)
K_v	h ⁻¹	0.0446 (0.0413 ... 0.0481)	Maximum likelihood, runs R1-R4 and R6-R9
$K_{v\theta}$	°C ⁻¹	0.132 (0.127 ... 0.137)	Maximum likelihood, runs R1-R4 and R6-R9
K_{vC}	g ⁻¹ L	0.074 (0.034 ... 0.113)	Maximum likelihood, runs R1-R4 and R6-R9
K_C	g L ⁻¹	0.0283	Tables supplied by professional brewer association
$K_{C\theta}$	°C ⁻¹	-0.0335	Tables supplied by professional brewer association
K_E	g L ⁻¹	25.5 (22.2 ... 29.2)	Maximum likelihood, runs R1-R4 and R6-R9
K_S	g L ⁻¹	3	Reference [11]
K_X	g L ⁻¹ (10 ⁶ cells mL ⁻¹) ⁻¹	0.145 (0.122 ... 0.172)	Maximum likelihood, runs R1-R4 and R6-R9
M_a	g mol ⁻¹	28.8	20% O ₂ + 80% N ₂ by volume
M_c	g mol ⁻¹	44	Chemical formula of CO ₂
p_{atm}	mbar	1013	760 mm Hg
R	mbar L mol ⁻¹ K ⁻¹	83.1	Perfect gas constant
$Y_{E/C}$	g g ⁻¹	1.028 (1.013 ... 1.043)	Reference [7]
$Y_{S/C}$	g g ⁻¹	1.884 (1.834 ... 1.934)	Reference [7]

Table 2. Numerical values of the parameters in the aroma production model

(In parenthesis: 95% confidence limits)

Source: maximum likelihood estimation based on data from runs R1-R4 and R6-R9

Parameter	Aroma compound (<i>i</i>)					
	ETA	ETX	IAA	IAL	PHL	DIA
σ_i	2.73	0.0201	0.224	8.08	4.78	0.106 (0.092 ... 0.125)
$W_{i,1}$	0.0426 (0.0386 ... 0.0470)	0.00027 (0.00023...0.00031)	0.0040 (0.0037 ... 0.0044)	1.91 (1.80 ... 2.04)	0.83 (0.75 ... 0.91)	0.0102 (0.0083 ... 0.0124)
$W_{i,2}$	0.148 (0.123 ... 0.172)	0.162 (0.126 ... 0.198)	0.143 (0.119 ... 0.167)	0	0.054 (0.026 ... 0.082)	0.176 (0.129 ... 0.222)
$W_{i,3}$	-0.838 (-1.001 ... -0.675)	-0.651 (-0.797 ... -0.506)	-0.754 (-0.876 ... -0.632)	-0.080 (-0.147 ... -0.012)	-0.11 (-0.22 ... -0.003)	0.203 (0.162 ... 0.255)
$W_{i,4}$	0	-0.045 (-0.066 ... -0.025)	-0.034 (-0.047 ... -0.021)	0.015 (0.008 ... 0.022)	0.011 (0.001 ... 0.021)	0.175 (0.110 ... 0.390)
$W_{i,5}$	0	0	0	0.052 (0.033 ... 0.070)	0.036 (0.001 ... 0.071)	NA
$W_{i,6}$	0.0041 (0.0015 ... 0.0066)	0.011 (0.005 ... 0.017)	0.0046 (-0.0007 ... 0.0099)	0.0040 (0.0018 ... 0.0062)	0.0052 (0.0020 ... 0.0084)	NA
$W_{i,7}$	0	0	0	-0.023 (-0.032 ... -0.013)	-0.018 (-0.032 ... -0.005)	NA
$W_{i,8}$	0	0	0.0046 (-0.0015 ... 0.0106)	0	0	NA

NA = not applicable

Table 3. Numerical values of the optimal control problem parameters.

Parameter	Units	Value	Parameter	Units	Value	Parameter	Units	Value
θ_{max}	°C	16	$K_{p\theta}$	h ⁻¹	5	W_{ETX}	none	1
θ_{min}	°C	10	K_{pp}	g L ⁻¹ h ⁻¹ mbar ⁻¹	5×10^{-4}	W_{IAA}	none	1
$\Phi_{\theta_{max}}$	°C h ⁻¹	0.5	n_t	none	49	W_{IAL}	none	1
$\Phi_{g_{max}}$	g L ⁻¹ h ⁻¹	2	p_{max}	mbar	1813	W_{PHL}	none	1
$A_{DIA,typ}$	mg L ⁻¹	0.1	S_{res}	g L ⁻¹	1	W_p	none	2×10^{-4}
$A_{ETA,org}$	mg L ⁻¹	2.5	$t_{f_{max}}$	h	200	W_t	none	0.1
$A_{ETX,org}$	mg L ⁻¹	0.02	t_{typ}	h	100	$X_{0_{min}}$	10 ⁶ cells mL ⁻¹	5
$A_{IAA,org}$	mg L ⁻¹	0.20	W_{θ}	none	2×10^{-4}	$X_{0_{max}}$	10 ⁶ cells mL ⁻¹	20
$A_{IAL,org}$	mg L ⁻¹	5	W_{DIA}	none	0.1			
$A_{PHL,org}$	mg L ⁻¹	4	W_{ETA}	none	1			

Table 4. Target ethanol and aroma compound concentrations

Beer sort	E_{trg} g L ⁻¹	$A_{ETA,trg}$ mg L ⁻¹	$A_{ETX,trg}$ mg L ⁻¹	$A_{IAA,trg}$ mg L ⁻¹	$A_{IAL,trg}$ mg L ⁻¹	$A_{PHL,trg}$ mg L ⁻¹
R5 ^a	40	15	0.115	1.0	77	34
B1 ^b	38	20	0.135	3.1	67	37
B2 ^b	48	18	0.086	1.6	96	47
B3 ^b	48	28	0.225	3.8	70	30
B4 ^b	40	28	0.125	4.1	62	22

^a Final ethanol and aroma concentrations measured in run R5

^b Ethanol and aroma concentrations measured in commercial beers

Figure legends

Figure 1. Alcoholic fermentation model validation. Data from run R5, not used for model identification. Measured values (o) and simulated values (—).

Figure 2. Aroma production model validation. Data from run R5, not used for model identification. Measured values (o) and simulated values (—).

Figure 3. Fermentation time reduction of an existing beer without changing the final aroma profile. **(A)** Constant operating conditions corresponding to run R5. **(B)** Time-varying operating condition determined by the dynamic optimisation algorithm. Top: aroma concentrations at the end of the alcoholic fermentation. Bottom: operating conditions for the alcoholic fermentation process. Target values (o), admissible range ($\cdot \cdot \cdot$) at $\pm 2A_{i,tol}$ and predicted values (—).

Figure 4. Different final aroma profiles obtained with the same yeast strain and wort. **(A)** Beer B2. **(B)** Beer B3. Top: aroma concentrations at the end of the alcoholic fermentation. Bottom: operating conditions for the alcoholic fermentation process. Target values (o), admissible range ($\cdot \cdot \cdot$) $\pm 2 A_{i,tol}$ and predicted values (—).

Figure 5. Aroma profiles impossible to achieve with the considered yeast strain and wort. **(A)** Beer B1. **(B)** Beer B4. Top: aroma concentrations at the end of the alcoholic fermentation. Bottom: operating conditions for the alcoholic fermentation process. Target values (o), admissible range ($\cdot \cdot \cdot$) at $\pm 2 A_{i,tol}$ and predicted values (—).

Figure 6. Sensitivity of the final aroma concentration and of the optimal control strategy to modelling errors. **(A)** The optimal control policy for beer B2 was applied without change to 20 possible model parameter sets. **(B)** The optimal control policy for beer B3 was recomputed for 20 possible model parameter sets. Top: aroma concentrations at the end of the alcoholic fermentation. Bottom: operating conditions for the alcoholic fermentation process. Target values (o), admissible range ($\cdot \cdot \cdot$) at $\pm 2 A_{i,tol}$ and 95% confidence intervals for the predicted values (■).

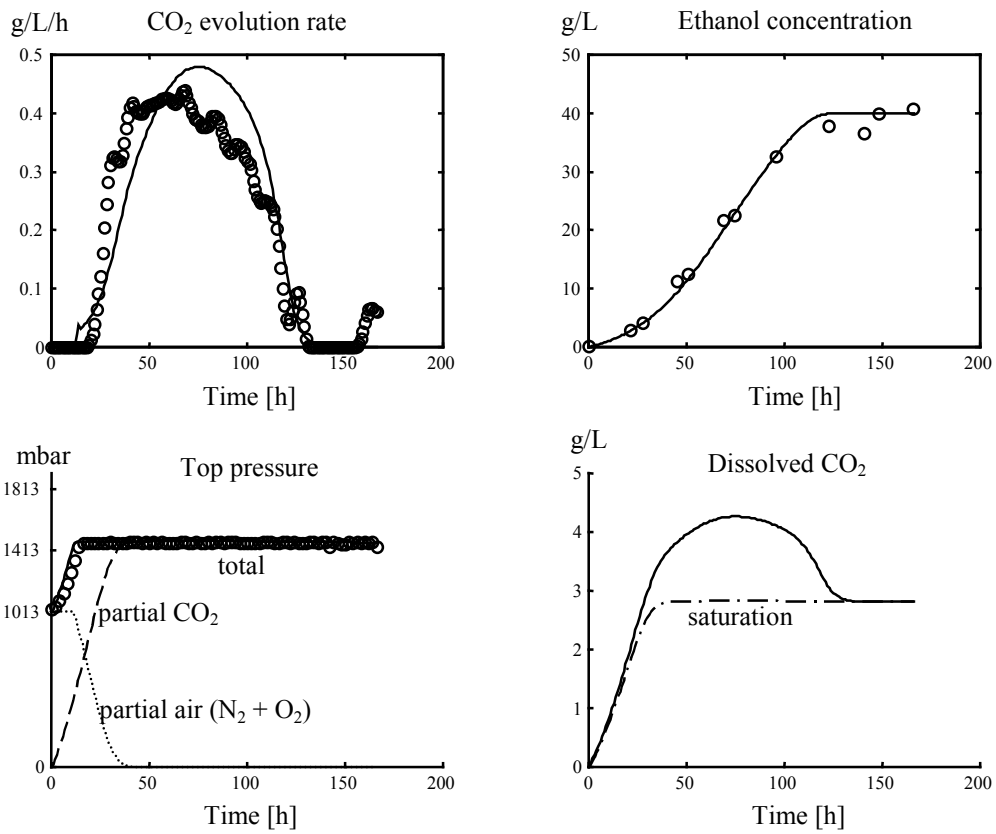


Figure 1

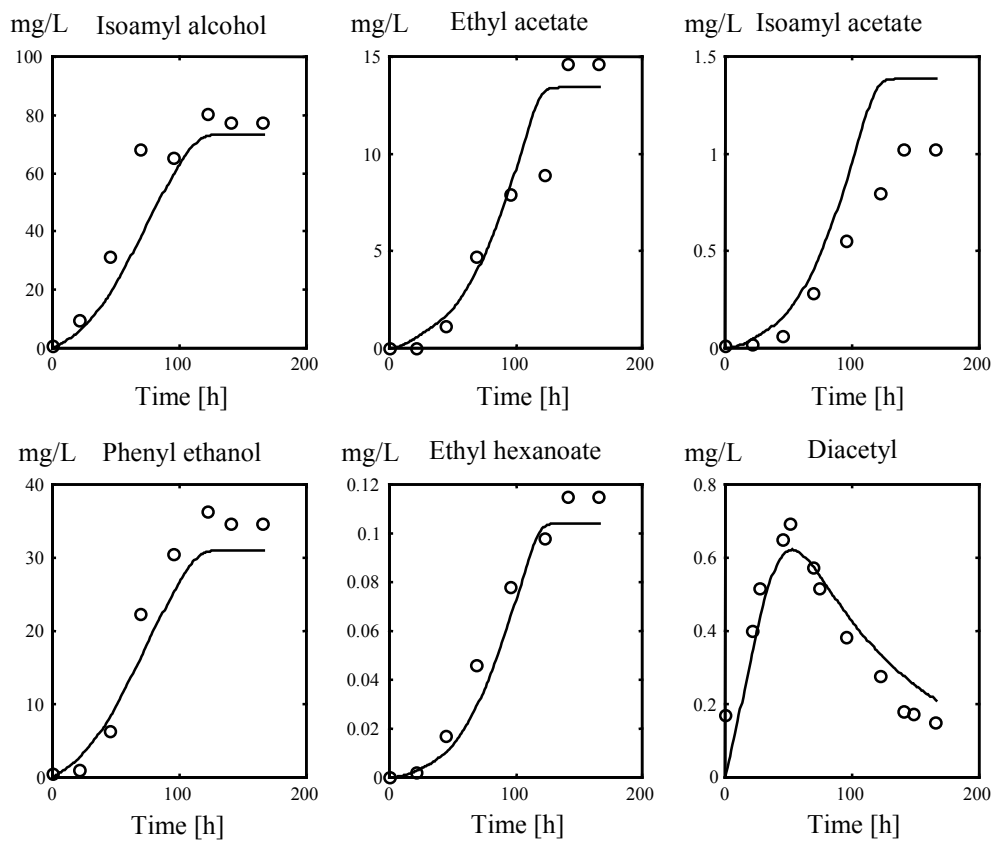


Figure 2

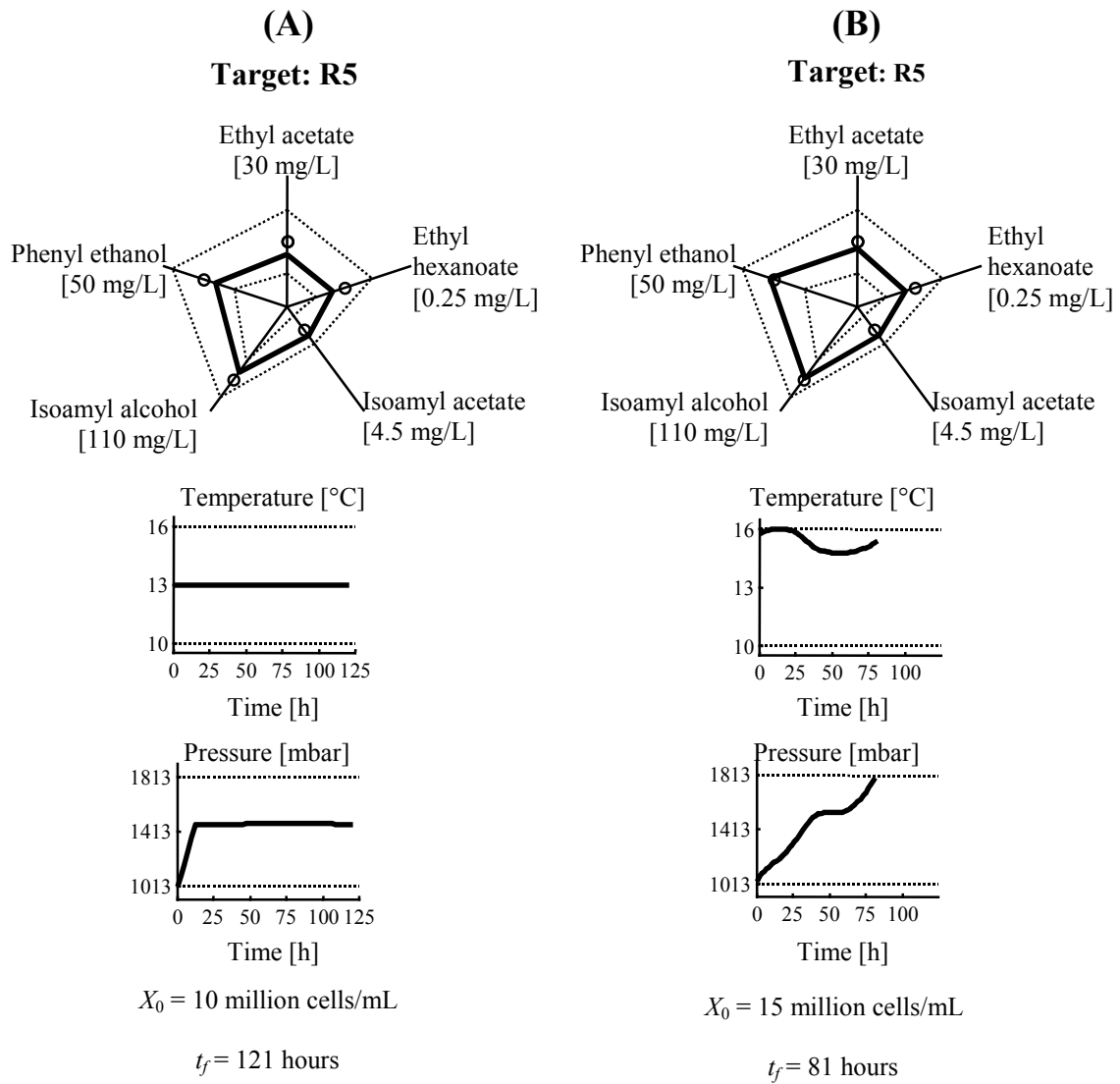


Figure 3.

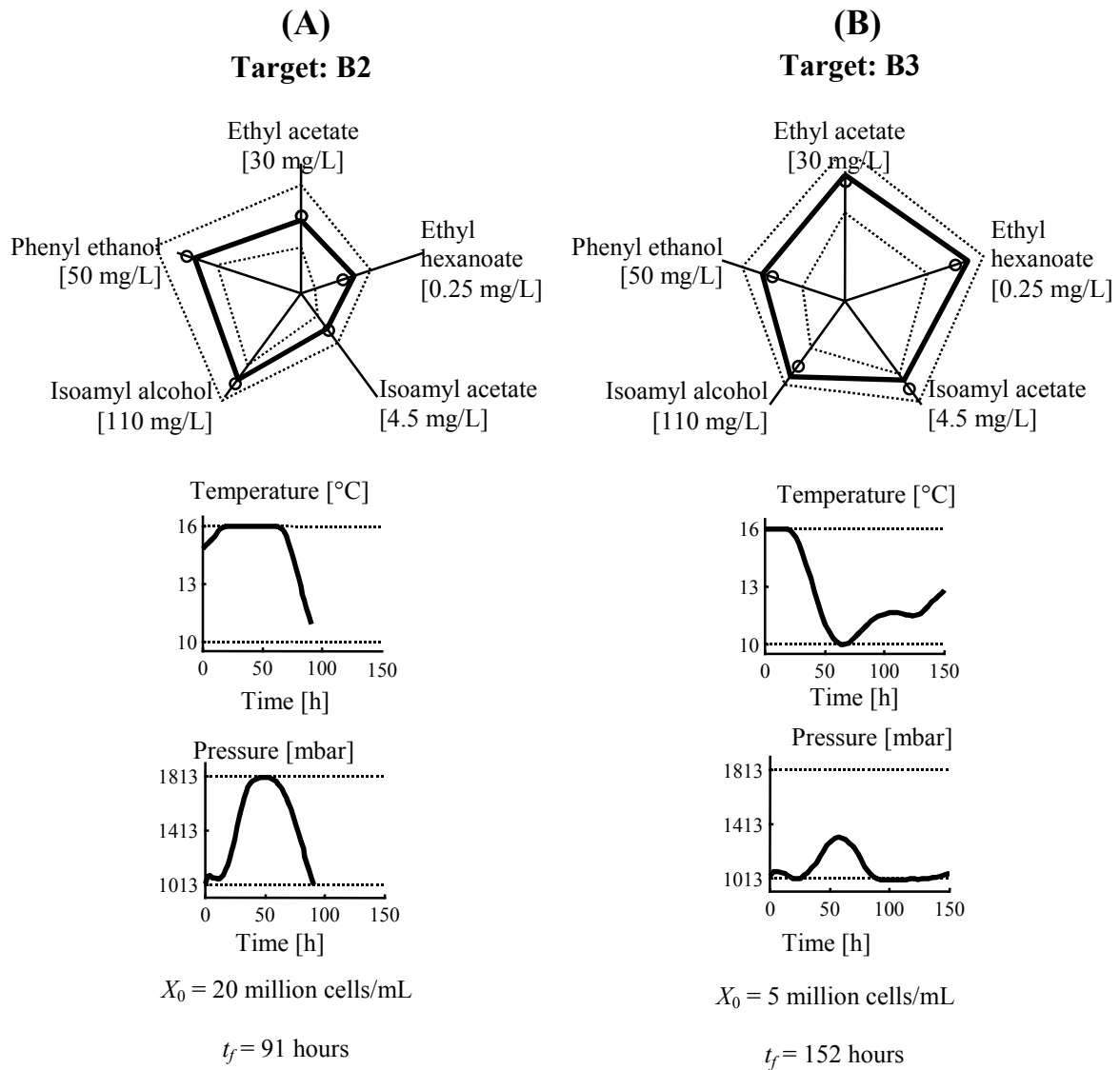


Figure 4.

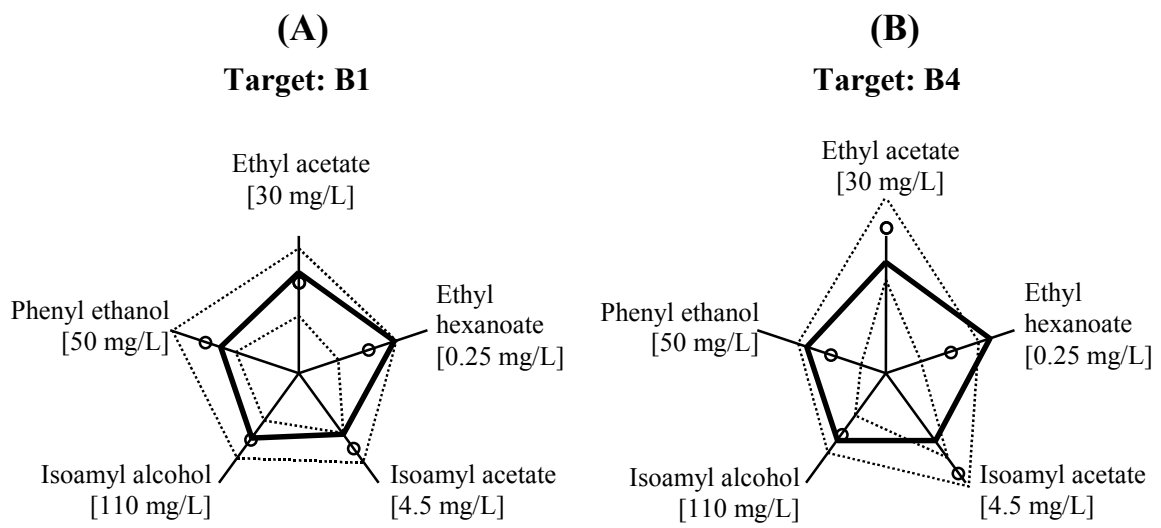


Figure 5.

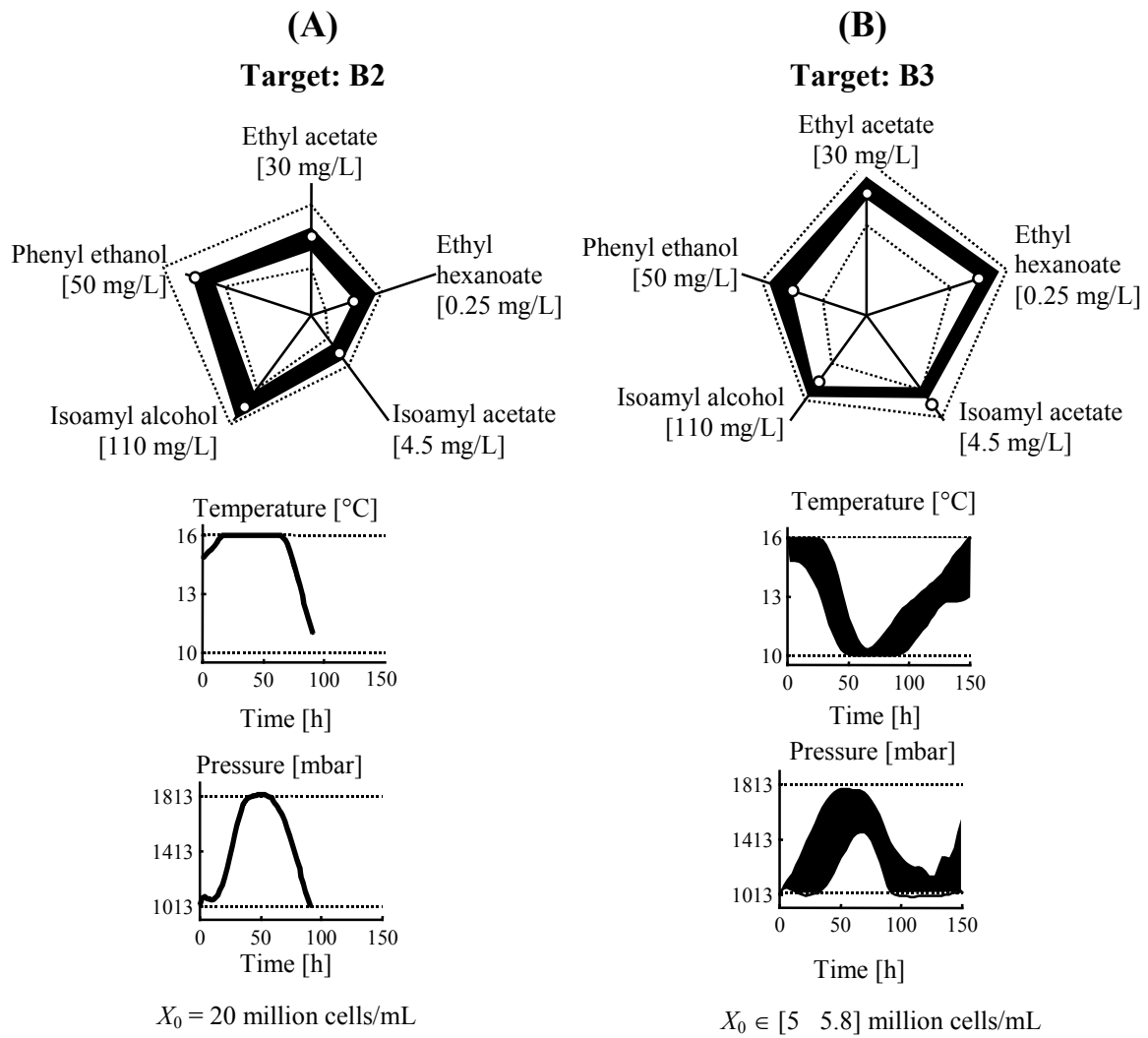


Figure 6.